Fracton Topological Phases from Strongly Coupled Spin Chains

Gábor B. Halász, Timothy H. Hsieh, and Leon Balents
Kavli Institute for Theoretical Physics, University of California, Santa Barbara, California 93106, USA
(Received 8 August 2017; published 20 December 2017)

We provide a new perspective on fracton topological phases, a class of three-dimensional topologically ordered phases with unconventional fractionalized excitations that are either completely immobile or only mobile along particular lines or planes. We demonstrate that a wide range of these fracton phases can be constructed by strongly coupling mutually intersecting spin chains and explain via a concrete example how such a coupled-spin-chain construction illuminates the generic properties of a fracton phase. In particular, we describe a systematic translation from each coupled-spin-chain construction into a parton construction where the partons correspond to the excitations that are mobile along lines. Remarkably, our construction of fracton phases is inherently based on spin models involving only two-spin interactions and thus brings us closer to their experimental realization.

DOI: 10.1103/PhysRevLett.119.257202

One of the most striking features of topologically ordered phases in two dimensions is the existence of quasiparticle excitations with fractional quantum numbers and fractional exchange statistics [1]. In three dimensions, this fractionalization attains an even more exotic character and has proven to be a vast and exciting frontier. For example, there are looplike excitations in addition to pointlike excitations, and the intricate braiding patterns exhibited by these looplike excitations are essential for characterizing the topological order [2,3].

Fracton topological phases are topologically ordered phases in three dimensions with a particularly extreme form of fractionalization [4–9]. In these phases, there are pointlike excitations that are either completely immobile or only mobile in a lower-dimensional subsystem, such as an appropriate line or plane. Remarkably, the restricted mobility of excitations has a purely topological origin and appears in translation-invariant systems without any disorder. In addition to being of fundamental interest from the perspective of topological phases, and providing an exciting disorder-free alternative to many-body localization [10,11], this phenomenology has important implications for quantum-information storage. Indeed, the immobility of excitations makes encoded quantum information more stable at finite temperature than in conventional topologically ordered phases [12,13].

In recent years, several different viewpoints have been presented on fracton topological phases. From a purely conceptual perspective, fracton phases can be understood by gauging classical spin models with particular subsystem symmetries [14,15] or in terms of generalized parton constructions with overlapping directional gauge constraints and/or interacting parton Hamiltonians [16]. While these approaches can be used to understand the generic properties of fracton phases, the concrete spin models they provide are far from realistic as they involve interactions between many spins at the same time. From a more practical perspective, fracton phases can be constructed by coupling orthogonal stacks of two-dimensional topologically ordered layers [17,18]. This approach can lead to more realistic spin models involving only two-spin interactions [19], although it is not immediately clear what kind of fracton phase is obtained from a generic construction.

In this Letter, we provide an understanding of fracton topological phases in terms of coupled spin chains and, along with it, a systematic route to construct realistic spin models hosting such fracton phases. This coupled-spin-chain construction is useful for three main reasons. First, like all coupled-chain (i.e., coupled-wire) constructions, it decomposes the system into its most basic building blocks, and dealing directly with these building blocks offers significant versatility in describing a rich variety of fracton phases. Second, the coupled-spin-chain constructions directly translate into generalized parton constructions, and the generic properties of the corresponding fracton phases can then be readily understood. For example, one can immediately identify the excitations with restricted mobility and their respective lower-dimensional subsystems (i.e., lines or planes). Third, the coupled-spin-chain constructions naturally give rise to fracton spin models involving only two-spin interactions, which are more amenable to a potential experimental implementation.

Fracton spin model.—Our coupled-spin-chain construction works for any $4n$-coordinated ($n \geq 2$) lattice with $2n$ spin-one-half degrees of freedom per site. For concreteness, however, we concentrate on the eight-coordinated ($n = 2$) body-centered-cubic (bcc) lattice, which is characterized by the (conventional) cubic lattice vectors $\mathbf{a}_{1,2,3}$ and the nearest-neighbor bond vectors $\mathbf{b}_{1,2,3,4}$ [see Fig. 1(a)].

In the concrete model, there are four spins $\sigma_{\mathbf{r},j}$ with flavors $j = 1, 2, 3, 4$ at each site $\mathbf{r}$ of the bcc lattice, and the Hamiltonian in terms of these spins reads

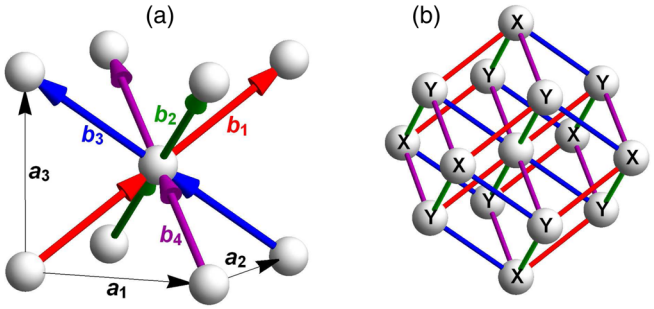

FIG. 1. Fracton spin model on the bcc lattice characterized by cubic lattice vectors $\mathbf{a}_{1,2,3}$ and bond vectors $\mathbf{b}_{1,2,3,4}$. (a) Nearest-neighbor terms of the model Hamiltonian H. Each term corresponding to a $j = 1$ (red), $j = 2$ (green), $j = 3$ (blue), or $j = 4$ (purple) bond acts on spin flavor j via σ^x at the tail and via σ^y at the head of the bond arrow. (b) Effective Hamiltonian $\tilde{H}$ in the strong-coupling limit. Each term $W_{\mathbf{r}}$ in $\tilde{H}$ is induced by nearest-neighbor terms (colored lines) in degenerate perturbation theory and is a product of eight spin operators $Y_{\tilde{\mathbf{r}}}$ at the corners of the basic bcc cube as well as six spin operators $X_{\tilde{\mathbf{r}}}$ at the apices of the square pyramids based on the faces of this cube. All sites $\tilde{\mathbf{r}}$ are marked by appropriate labels.

$$H = -J\sum_j \sum_{\langle \mathbf{r},\mathbf{r}'\rangle_j} \sigma^x_{\mathbf{r},j}\sigma^y_{\mathbf{r}',j} - \lambda J \sum_{\mathbf{r}} \sum_{\langle j,j'\rangle} \sigma^z_{\mathbf{r},j}\sigma^z_{\mathbf{r},j'}, \quad (1)$$

where $\langle j, j'\rangle$ implies a summation over all pairs of spins at the same site, and $\langle \mathbf{r}, \mathbf{r}'\rangle_j$ implies a summation over all j bonds ($j = 1, 2, 3, 4$) such that the arrow in Fig. 1(a) points from $\mathbf{r}$ to $\mathbf{r}'$ at each bond. The first (nearest-neighbor) term describes decoupled spin chains of the four spin flavors along the $\langle 111\rangle$ directions traced out by strings of the four corresponding bond types, while the second (on-site) term introduces a coupling between spin chains of distinct spin flavors intersecting at any site. Note that the individual (decoupled) spin chains are both critical and macroscopically degenerate.

In the strong-coupling regime ($\lambda \gg 1$), the four spins $\sigma_{\mathbf{r},j}$ at each site $\mathbf{r}$ are locked together by the on-site terms, and thus $\sigma^z_{\mathbf{r},j} = \sigma^z_{\mathbf{r},j'}$ for all j and j'. The local Hilbert space is then captured by a single effective spin $\Sigma_{\mathbf{r}}$ as its two states can be characterized by $\Sigma^z_{\mathbf{r}} = \sigma^z_{\mathbf{r},j} = \pm 1$. For $\lambda \to \infty$, these degenerate local states give rise to an exponentially large ground-state degeneracy. However, if λ is finite, the nearest-neighbor terms select particular superpositions of these ground states by inducing a low-energy Hamiltonian within the ground-state subspace in terms of the effective spin components

$$\begin{aligned} X_{\mathbf{r}} &\equiv \Sigma^x_{\mathbf{r}} = \sigma^x_{\mathbf{r},1}\sigma^x_{\mathbf{r},2}\sigma^x_{\mathbf{r},3}\sigma^x_{\mathbf{r},4} = -\sigma^y_{\mathbf{r},1}\sigma^y_{\mathbf{r},2}\sigma^x_{\mathbf{r},3}\sigma^x_{\mathbf{r},4} = \ldots, \\ Y_{\mathbf{r}} &\equiv \Sigma^y_{\mathbf{r}} = \sigma^y_{\mathbf{r},1}\sigma^x_{\mathbf{r},2}\sigma^x_{\mathbf{r},3}\sigma^x_{\mathbf{r},4} = \sigma^x_{\mathbf{r},1}\sigma^y_{\mathbf{r},2}\sigma^x_{\mathbf{r},3}\sigma^x_{\mathbf{r},4} = \ldots, \\ Z_{\mathbf{r}} &\equiv \Sigma^z_{\mathbf{r}} = \sigma^z_{\mathbf{r},1} = \sigma^z_{\mathbf{r},2} = \sigma^z_{\mathbf{r},3} = \sigma^z_{\mathbf{r},4}. \end{aligned} \quad (2)$$

For our bcc model in Eq. (1), the lowest-order nontrivial Hamiltonian term $W_{\mathbf{r}}$ arises at order 32 in degenerate perturbation theory (see the Supplemental Material [20]) and is a product of 14 effective spin operators [see Fig. 1(b)]. Ignoring any trivial (i.e., constant) terms, the effective Hamiltonian at this order is then $\tilde{H} = \sum_{\mathbf{r}} W_{\mathbf{r}}$, where

$$W_{\mathbf{r}} \sim \frac{J}{\lambda^{31}} \prod_{\pm} X_{\mathbf{r}\pm\mathbf{a}_1} X_{\mathbf{r}\pm\mathbf{a}_2} X_{\mathbf{r}\pm\mathbf{a}_3} Y_{\mathbf{r}\pm\mathbf{b}_1} Y_{\mathbf{r}\pm\mathbf{b}_2} Y_{\mathbf{r}\pm\mathbf{b}_3} Y_{\mathbf{r}\pm\mathbf{b}_4}. \quad (3)$$

Since $[W_{\mathbf{r}}, W_{\mathbf{r}'}] = 0$ for all $\mathbf{r}$ and $\mathbf{r}'$, the Hamiltonian $\tilde{H}$ corresponds to a commuting-projector model, where each eigenstate is characterized by $W_{\mathbf{r}} = \pm 1$. Furthermore, the only nontrivial terms arising at higher orders of perturbation theory are products of $W_{\mathbf{r}}$, and this commuting-projector model thus captures an entire strong-coupling phase $\lambda > \lambda_C$ above a critical coupling strength λ_C.

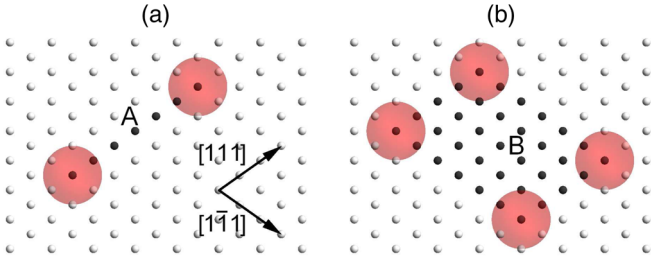

FIG. 2. One-dimensional (a) and zero-dimensional (b) excitations in the $(10\bar{1})$ plane of our bcc model. In each case, the excitations are (schematically) located within the red circles and are created by the operator $\prod_{\mathbf{r}\in A,B} Z_{\mathbf{r}}$ over the sites $\mathbf{r} \in A, B$ marked by black dots.

This strong-coupling phase of the model in Eq. (1) is identified as a type-I fracton phase [14], which is characterized by the following (closely related) features. First of all, there is a ground-state degeneracy that scales as $\sim 2^L$ with the linear system dimension L due to the planar conservation laws $\prod_{\mathbf{r}\in\{110\}} W_{\mathbf{r}} = \text{const}$ within the $\{110\}$ planes of the lattice [21]. For a product $\prod_{\mathbf{r}\in R\subset\{110\}} W_{\mathbf{r}}$ within a finite region R of a $\{110\}$ plane, the boundary of the region then corresponds to a string logical operator, and the excitations at the end points of such a string ∂R are only mobile within the given $\{110\}$ plane. Moreover, there is a string logical operator $\prod_{\mathbf{r}\in A} Z_{\mathbf{r}}$ along each $\langle 111\rangle$ direction of the lattice, and the excitations at the end points of such a string A are only mobile along the given $\langle 111\rangle$ direction [see Fig. 2(a)]. Finally, these strings can be assembled into membrane logical operators $\prod_{\mathbf{r}\in B} Z_{\mathbf{r}}$ within parallelepipeds spanned by two distinct $\langle 111\rangle$ directions (e.g., the $[111]$ and the $[1\bar{1}1]$ directions), and the excitations at the corners of such a parallelepiped B are completely immobile [see Fig. 2(b)].

Parton decomposition.—The effective spin Hamiltonian $\tilde{H}$ has an exact noninteracting parton construction. Indeed, the spins $\Sigma_{\mathbf{r}}$ can be decomposed into clusters of partons that are individually governed by a noninteracting Hamiltonian

but are also subject to gauge constraints that recombine them into their parent spins. Such parton constructions are commonly used to capture strongly correlated spin phases, including spin liquids, on a variational level [22].

For the eight-coordinated bcc lattice, it is a natural choice [23] to decompose each spin $\Sigma_{\mathbf{r}}$ into eight Majorana fermions (partons) $\gamma_{\mathbf{r},j}$ and $\hat{\gamma}_{\mathbf{r},j}$ with flavors $j = 1, 2, 3, 4$ and to assign these eight partons to the eight respective bonds around the site $\mathbf{r}$ [see Fig. 3(a)]. The two Majorana fermions at each bond then form a complex fermion, which is demanded to be in an occupied or an unoccupied state, and the parton state is simply the direct product of all these local states. Formally, the parton state is the ground state of the noninteracting Hamiltonian

$$\mathcal{H} = \sum_{j} \sum_{\langle \mathbf{r},\mathbf{r}' \rangle_j} i\nu_{\mathbf{r},\mathbf{r}'} \gamma_{\mathbf{r},j} \hat{\gamma}_{\mathbf{r}',j}, \tag{4}$$

where $\nu_{\mathbf{r},\mathbf{r}'} = \pm 1$ determines whether the complex fermion at the bond $\langle \mathbf{r}, \mathbf{r}' \rangle_j$ is occupied or unoccupied.

Since the parton decomposition increases the local Hilbert space at each site, the partons must be reconciled with their parent spins by means of appropriate gauge constraints. Following Ref. [16], we capture our type-I fracton phase by imposing the overlapping directional gauge constraints

$$G_{\mathbf{r},j,j'} = \gamma_{\mathbf{r},j} \gamma_{\mathbf{r},j'} \hat{\gamma}_{\mathbf{r},j} \hat{\gamma}_{\mathbf{r},j'} = 1. \tag{5}$$

These gauge constraints are indeed directional as each of them only acts on partons in a particular $\{110\}$ plane and overlapping as any two such planes intersect along a particular $\langle 111 \rangle$ direction. We also note that there are three independent gauge constraints at each site which correctly reconcile eight Majorana fermions with a single spin.

The three components of the spin $\Sigma_{\mathbf{r}}$ are identified with the three inequivalent gauge-invariant operators

$$\begin{aligned} X_{\mathbf{r}} &= \gamma_{\mathbf{r},1}\gamma_{\mathbf{r},2}\gamma_{\mathbf{r},3}\gamma_{\mathbf{r},4} = -\hat{\gamma}_{\mathbf{r},1}\hat{\gamma}_{\mathbf{r},2}\gamma_{\mathbf{r},3}\gamma_{\mathbf{r},4} = \ldots, \\ Y_{\mathbf{r}} &= \hat{\gamma}_{\mathbf{r},1}\gamma_{\mathbf{r},2}\gamma_{\mathbf{r},3}\gamma_{\mathbf{r},4} = \gamma_{\mathbf{r},1}\hat{\gamma}_{\mathbf{r},2}\gamma_{\mathbf{r},3}\gamma_{\mathbf{r},4} = \ldots, \\ Z_{\mathbf{r}} &= i\hat{\gamma}_{\mathbf{r},1}\gamma_{\mathbf{r},1} = i\hat{\gamma}_{\mathbf{r},2}\gamma_{\mathbf{r},2} = i\hat{\gamma}_{\mathbf{r},3}\gamma_{\mathbf{r},3} = i\hat{\gamma}_{\mathbf{r},4}\gamma_{\mathbf{r},4}, \end{aligned} \tag{6}$$

where the equivalent expressions of each spin component are related by the gauge constraints $G_{\mathbf{r},j,j'}$. Each term $W_{\mathbf{r}}$ in the spin Hamiltonian $\tilde{H}$ is then readily written in terms of the partons and decomposes into a product of 32 bond-fermion operators $i\gamma_{\mathbf{r},j}\hat{\gamma}_{\mathbf{r}',j}$ in Eq. (4) [see Fig. 3(b)]. Since the terms $W_{\mathbf{r}}$ also commute with the gauge constraints, the exact eigenstates of the spin Hamiltonian $\tilde{H}$ are thus obtained from those of the (noninteracting) parton Hamiltonian $\mathcal{H}$ by enforcing the gauge constraints via appropriate projections.

From a comparison of Figs. 1 and 3, there is clearly an intimate connection between the coupled-spin-chain construction in Eq. (1) and the parton construction in Eq. (4). Indeed, the spin-combination rules in Eq. (2) for obtaining the effective low-energy Hamiltonian $\tilde{H}$ in degenerate perturbation theory are identical to the corresponding parton-decomposition rules in Eq. (6) via the substitutions $\sigma^x_{\mathbf{r},j} \leftrightarrow \gamma_{\mathbf{r},j}$, $\sigma^y_{\mathbf{r},j} \leftrightarrow \hat{\gamma}_{\mathbf{r},j}$, and $\sigma^z_{\mathbf{r},j} \leftrightarrow i\hat{\gamma}_{\mathbf{r},j}\gamma_{\mathbf{r},j}$. This connection can be understood by means of the Jordan-Wigner transformation

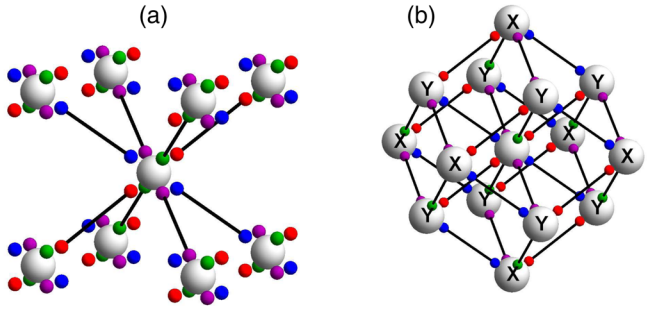

FIG. 3. Exact parton construction of our bcc model. (a) Each spin $\Sigma_{\mathbf{r}}$ (large white sphere) is decomposed into eight Majorana fermions (colored dots) at the bonds around the site $\mathbf{r}$: four $\gamma_{\mathbf{r},j}$ above $\mathbf{r}$ and four $\hat{\gamma}_{\mathbf{r},j}$ below $\mathbf{r}$ with flavors $j = 1$ (red), $j = 2$ (green), $j = 3$ (blue), and $j = 4$ (purple). Each bond is occupied by two Majorana fermions $\gamma_{\mathbf{r},j}$ and $\hat{\gamma}_{\mathbf{r}',j}$ that are in a state characterized by the bond-fermion operator $i\gamma_{\mathbf{r},j}\hat{\gamma}_{\mathbf{r}',j} = \pm 1$ (black line). (b) Decomposition of each term $W_{\mathbf{r}}$ in the effective spin Hamiltonian $\tilde{H}$ [see Fig. 1(b)] into a product of bond-fermion operators (black lines).

$$\begin{pmatrix} \sigma^x_{\mathbf{r},j} \\ \sigma^y_{\mathbf{r},j} \end{pmatrix} = \left(\prod_{\mathbf{r}'<\mathbf{r}} \prod_{j'} \sigma^z_{\mathbf{r}',j'} \prod_{j'<j} \sigma^z_{\mathbf{r},j'} (i\sigma^z_{\mathbf{r},j})^{j-1} \right) \begin{pmatrix} \gamma_{\mathbf{r},j} \\ \hat{\gamma}_{\mathbf{r},j} \end{pmatrix},$$

$$\sigma^z_{\mathbf{r},j} = i\hat{\gamma}_{\mathbf{r},j}\gamma_{\mathbf{r},j}, \tag{7}$$

where the additional factor $(i\sigma^z_{\mathbf{r},j})^{j-1}$ with respect to the standard form is a local spin rotation. Within the low-energy subspace characterized by $\Sigma_{\mathbf{r}}$, the Jordan-Wigner strings in the large parentheses then disappear due to the spin-locking constraints $\sigma^z_{\mathbf{r},j}\sigma^z_{\mathbf{r},j'} = 1$ or, equivalently, due to the corresponding gauge constraints $G_{\mathbf{r},j,j'} = 1$. We emphasize, however, that this connection is restricted to the low-energy subspace and that it would thus be incorrect to argue for Eq. (4) by directly substituting Eq. (7) into Eq. (1).

Extended fracton phase.—As discussed in Ref. [16], parton constructions can be used to understand the generic properties of fracton phases. In general, a strongly correlated spin phase is characterized by its parton construction via the invariant gauge group (IGG), which consists of all gauge transformations (i.e., generic products of local gauge constraints) that commute with the parton Hamiltonian.

For a type-I fracton phase, the IGG is generically $\mathbb{Z}_2^N$ with $N \sim L$ due to the presence of planar IGG elements that

are related to the planar conservation laws of the corresponding spin model [16]. For our bcc construction, in particular, there is a planar IGG element for each $\{110\}$ plane as the product of all $G_{\mathbf{r},j,j'}$ in a $\{110\}$ plane spanned by a net of j and j' bonds commutes with $\mathcal{H}$ in Eq. (4). The partons themselves can then be identified with the excitations that are only mobile along particular $\langle 111\rangle$ directions. Indeed, since each parton $\gamma_{\mathbf{r},j}$ ($\hat{\gamma}_{\mathbf{r},j}$) anticommutes with three planar IGG elements containing $G_{\mathbf{r},j,j'}$ with $j' \neq j$, it is constrained to move along the intersection of the three corresponding planes, which is a $\langle 111\rangle$ direction traced out by a string of j bonds.

Importantly, the parton construction is valid beyond the exactly solvable model $\tilde{H}$. In fact, any sufficiently weak local perturbation that commutes with all the IGG elements can be added to Eq. (4) while leaving the projected parton ground state in the original fracton phase. In addition to the terms $i\gamma_{\mathbf{r},j}\hat{\gamma}_{\mathbf{r}+\mathbf{b}_j,j}$ already present, the generic quadratic terms appearing are then $i\tilde{\gamma}_{\mathbf{r},j}\tilde{\gamma}_{\mathbf{r}+x\mathbf{b}_j,j}$, where x is an arbitrary integer, and $\tilde{\gamma}_{\mathbf{r},j}$ is either $\gamma_{\mathbf{r},j}$ or $\hat{\gamma}_{\mathbf{r},j}$. In turn, these generic terms lead to nontrivial parton dispersions along the respective $\langle 111\rangle$ directions of motion. While the resulting parton ground state does not correspond to an exactly solvable spin model, it can be used as the starting point of a variational description.

Generalized constructions.—Our coupled-spin-chain construction is extremely versatile and readily generalizes to a rich variety of fracton phases. First, it can be defined on any $4n$-coordinated ($n \geq 2$) lattice with $2n$ spins $\sigma_{\mathbf{r},j=1,\ldots,2n}$ at each site $\mathbf{r}$. Second, the intersecting spin chains can be embedded in the lattice in many different ways. In particular, they do not have to follow straight lines and might even connect back into themselves to form closed loops.

Formally, the Hamiltonian is Eq. (1) for any such coupled-spin-chain construction, where the different bond types are assigned to the given lattice in a particular way. It is crucial that there are precisely two bonds of each type j around each site $\mathbf{r}$ at which the two corresponding terms act with spin operators $\sigma^x_{\mathbf{r},j}$ and $\sigma^y_{\mathbf{r},j}$, respectively. Two examples of such generalized constructions are presented in Fig. 4(a) on a primitive hexagonal lattice and on a cubic lattice formed by corner-sharing octahedra. For each construction, there is a type-I fracton phase in the strong-coupling limit, and the independent terms $W_{\mathbf{r}}$ of the effective strong-coupling Hamiltonian $\tilde{H}$ are given in Fig. 4(b). Remarkably, the type-I fracton phase of the second construction is captured by the X-cube model [14].

Moreover, the fracton phase in the strong-coupling limit can be readily analyzed without obtaining the concrete form of the effective Hamiltonian $\tilde{H}$. Because of the connection between the coupled-spin-chain construction and the parton construction, the terms $W_{\mathbf{r}}$ in $\tilde{H}$ necessarily decompose into products of appropriate bond-fermion operators when written in terms of the partons. The fracton phase is then captured by the noninteracting parton Hamiltonian in Eq. (4), where the different bond types are assigned to the lattice in the same way as in Eq. (1). For such a generalized parton construction, the IGG elements are products of gauge constraints $G_{\mathbf{r},j,j'}$ along nets of j and j' bonds, while the partons themselves correspond to excitations that are mobile along respective strings of j bonds (i.e., the individual spin chains).

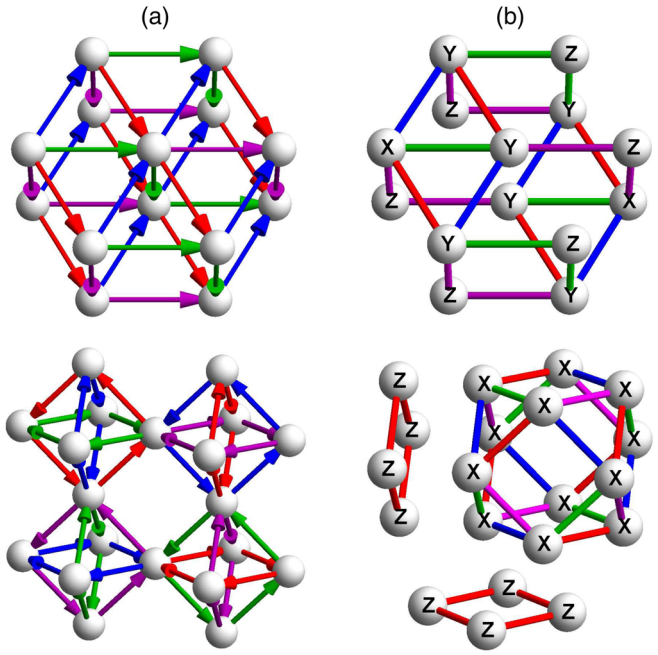

FIG. 4. Coupled-spin-chain constructions (a) and effective strong-coupling Hamiltonians (b) capturing type-I fracton phases on two different lattices. The notation is taken from Fig. 1. For the second construction, the strong-coupling Hamiltonian has three independent terms and corresponds to the X-cube model [14].

Summary and outlook.—We have provided a general framework for describing fracton topological phases in terms of an interpenetrating set of spin chains that are strongly coupled at their intersection points. It is clear from the examples presented that this construction can easily describe many different fracton phases by spin models involving only two-spin interactions. This work covers the strong-coupling limit of these spin models, while the weak-coupling limit and the quantitative domain of the fracton phase in the strong-coupling regime (i.e., the value of λ_C) remain to be understood.

Our construction of fracton phases is analogous to how the toric-code model is obtained in the spatially anisotropic limit of the Kitaev honeycomb model [1]. Indeed, if we form two pairs out of the four spin flavors in Eq. (1) and only introduce couplings within each pair, we obtain two orthogonal stacks of two-dimensional topologically ordered layers; see the Supplemental Material [20]. The fracton phase is then recovered by including the remaining

couplings between the two orthogonal stacks [19]. In a conceptual sense, the coupled-layer models of fracton phases introduced in Refs. [17,18] are thus an intermediate step between our coupled-spin-chain models and the commuting-projector models in Ref. [14].

Finally, it follows from our work that parton constructions describing fracton phases can be generally converted into appropriate spin models. While the noninteracting parton constructions in this work give rise to coupled-spin-chain models involving two-spin interactions, the interacting parton constructions in Ref. [16] translate into more general spin models involving four-spin interactions. Remarkably, these parton constructions describe both type-I and type-II fracton phases, characterized by immobile excitations at the corners of membrane and fractal operators, respectively [24]. Our formalism thus brings us one step closer to realizing these highly unconventional topological phases in the laboratory.

G. B. H. and T. H. H. are supported by the Gordon and Betty Moore Foundation's EPiQS Initiative through Grant No. GBMF4304. L. B. was supported by the National Science Foundation under Grant No. NSF DMR1506119.

[1] A. Y. Kitaev, Ann. Phys. (Amsterdam) **321**, 2 (2006).
[2] C. Wang and M. Levin, Phys. Rev. Lett. **113**, 080403 (2014).
[3] S. Jiang, A. Mesaros, and Y. Ran, Phys. Rev. X **4**, 031048 (2014).
[4] C. Chamon, Phys. Rev. Lett. **94**, 040402 (2005).
[5] S. Bravyi, B. Leemhuis, and B. M. Terhal, Ann. Phys. (Amsterdam) **326**, 839 (2011).
[6] J. Haah, Phys. Rev. A **83**, 042330 (2011).
[7] B. Yoshida, Phys. Rev. B **88**, 125122 (2013).
[8] S. Vijay, J. Haah, and L. Fu, Phys. Rev. B **92**, 235136 (2015).
[9] M. Pretko, Phys. Rev. B **95**, 115139 (2017).
[10] I. H. Kim and J. Haah, Phys. Rev. Lett. **116**, 027202 (2016).
[11] A. Prem, J. Haah, and R. Nandkishore, Phys. Rev. B **95**, 155133 (2017).
[12] S. Bravyi and J. Haah, Phys. Rev. Lett. **107**, 150504 (2011).
[13] S. Bravyi and J. Haah, Phys. Rev. Lett. **111**, 200501 (2013).
[14] S. Vijay, J. Haah, and L. Fu, Phys. Rev. B **94**, 235157 (2016).
[15] D. J. Williamson, Phys. Rev. B **94**, 155128 (2016).
[16] T. H. Hsieh and G. B. Halász, Phys. Rev. B **96**, 165105 (2017).
[17] H. Ma, E. Lake, X. Chen, and M. Hermele, Phys. Rev. B **95**, 245126 (2017).
[18] S. Vijay, arXiv:1701.00762.
[19] K. Slagle and Y. B. Kim, Phys. Rev. B **96**, 165106 (2017).
[20] See the Supplemental Material at http://link.aps.org/supplemental/10.1103/PhysRevLett.119.257202 for a more detailed description of degenerate perturbation theory and the relation of our work to coupled-layer constructions.
[21] In fact, for an $L \times L \times L$ system, a detailed analysis shows that the ground-state degeneracy is 2^{12L-10}.
[22] X.-G. Wen, Phys. Rev. B **65**, 165113 (2002).
[23] X.-G. Wen, Phys. Rev. Lett. **90**, 016803 (2003).
[24] The coupled-spin-chain models in this work typically describe type-I fracton phases as they have excitations that are mobile along the individual spin chains. Nevertheless, type-II fracton phases with only immobile excitations can, in principle, also be captured if all spin chains form closed loops. This extension of our work is currently in progress.